RESEARCH ARTICLE
doi: 10.2306/scienceasia1513-1874.2025.s026

ScienceAsia 51S (2): 2025: ID 2025s026: **1–10**

Petrotectonics of plutonic rocks in the eastern Mae Chan area, Chiang Rai, northern Thailand

Patcharin Kosuwan Jundee[a,*], Burapha Phajuy[a], Yuenyong Panjasawatwong[a], Prinya Putthapiban[b], Panjai Saraphanchotwitthaya[c], Panawat Watthanapond[d], Ekkachak Chandon[b], Piyanat Arin[a]

[a] Department of Geological Sciences, Faculty of Science, Chiang Mai University, Chiang Mai 50200 Thailand
[b] Division of Geoscience, School of Interdisciplinary Studies, Mahidol University, Kanchanaburi Campus, Kanchanaburi 71150 Thailand
[c] Department of Mineral Resources, Bangkok 10400 Thailand
[d] Department of Geology, Faculty of Science, Chulalongkorn University, Bangkok 10330 Thailand

[*]Corresponding author, e-mail: patcharinkosuwan.j@cmu.ac.th

Received 12 Nov 2024, Accepted 9 Nov 2025
Available online 20 Dec 2025

ABSTRACT: The plutonic rocks in Doi Pha Rua and Doi Sak, the eastern part of Tha Khao Pluek Sub-District, Mae Chan District, Chiang Rai Province, exhibit compositions ranging from felsic to mafic rocks. Petrography and geochemistry are essential tools for classifying rocks into four magmatic groups. Group I is monzogranite, granodiorite, and tonalite, with titanite as a minor constituent. They are peraluminous and have medium-K transitional to high-K calc-alkaline affinities that show both I-type and S-type. Their N-MORB-normalized multi-element patterns exhibit LILE enrichment and a negative Nb anomaly, which are typical of magmas formed at active continental margins. Group II is tonalite, with titanite as a minor constituent. They are peraluminous, tholeiitic series, characteristic of I-type granite. Group II does not exhibit a negative Nb anomaly in N-MORB normalized multi-element patterns and might have occurred in a post-collision environment. Group III is cumulate gabbro and tholeiitic series. Their chondrite-normalized REE patterns show positive Eu anomalies. Group IV is microgabbro and has chondrite-normalized REE and N-MORB normalized multi-element patterns that are very similar to those of Group I. Groups I and II are informative to tectonic environments of formation, while Group III and IV are cumulative (not represent magma) and isotropic, respectively. One Group IV sample is meaningless for interpretation. The Group I is volcanic arc granite, and Group II might have been post-collision granite. The Mae Chan granitic pluton is a part of Eastern Granitic Belt (EGB) and represents magmatism along the boundary between the Sukhothai Arc and the Inthanon Zone.

KEYWORDS: eastern Mae Chan area, I- and S-type granite, petrotectonics, active continental margin, syn-collision, post-collision

INTRODUCTION

The intrusive rocks in SE Asia region have been studied by many researchers and focused mainly on granitic rocks because they are voluminous and related to economic minerals such as tin-tungsten, precious metals, and rare earth element (REE) minerals [1–6]. The granitic rocks in Thailand and SE Asia are separated into three granitic belts: the Western (SW Thailand–eastern Myanmar), the Central Main Range (central north Thailand–western Malaysia), and the Eastern (Laos, eastern Thailand, and eastern Malaysia), based on their distribution and geochemistry, as illustrated in Fig. 1a [7–10]. The western granitic belt (WGB) is distributed along the Thai-Myanmar border, Phuket Island (Thailand), and Aceh and Sumatra islands (Indonesia), and consists of granite, monzonite, and granodiorite. The WGB whole-rock geochemistry is ferroan, alkaline to calcic alkaline, and peraluminous, and shows S-type affinity. The tectonic settings of formation were syn-collision and post-collision [6]. The central main range granitic belt (CGB) is the main granitoid in Thailand and SE Asia and occurs as plutons with a continuous north-south orientation, underlying almost all northern-central and peninsular Thailand, the main range of Malaysia, and the Bangka, Singkep, and Tuju Islands of Indonesia [2, 4, 10, 11]. The CGB in northern Thailand is divided into two sub-belts. The western sub-belt is situated in the southern part of Mae Hong Son Province along the Thai-Myanmar border and consists of composite plutons (Mae Sariang complex) extending from Pai District through Samoeng, Mae Chaem, and Hot Districts and Doi Inthanon Mountains, Chiang Mai Province, to the western part of Tak Province. The eastern sub-belt comprises the Mae Chan pluton in Chiang Rai Province, the Fang-Mae Suai-Wiang Pa Pao batholith [12] in Chiang Mai Province, and the Khuntan batholith in Lamphun Province. The CGB rocks comprise granite, granodiorite, and monzodiorite, and exhibit high-K calc-alkaline, peraluminous, and S-type signatures. Their absolute ages in northern Thailand, determined by $^{40}Ar/^{39}Ar$ dating, are 220–180 Ma (Late Triassic–Middle Jurassic) [2]. The zircon U-Pb age of granite in the Mae Suai area, Chiang Rai Province is 220+1 (Late Triassic) [13]. Eastern Granitic Belt (EGB) is distributed from central to eastern Thailand, along the edge of the Korat Plateau. The EGB rocks con-

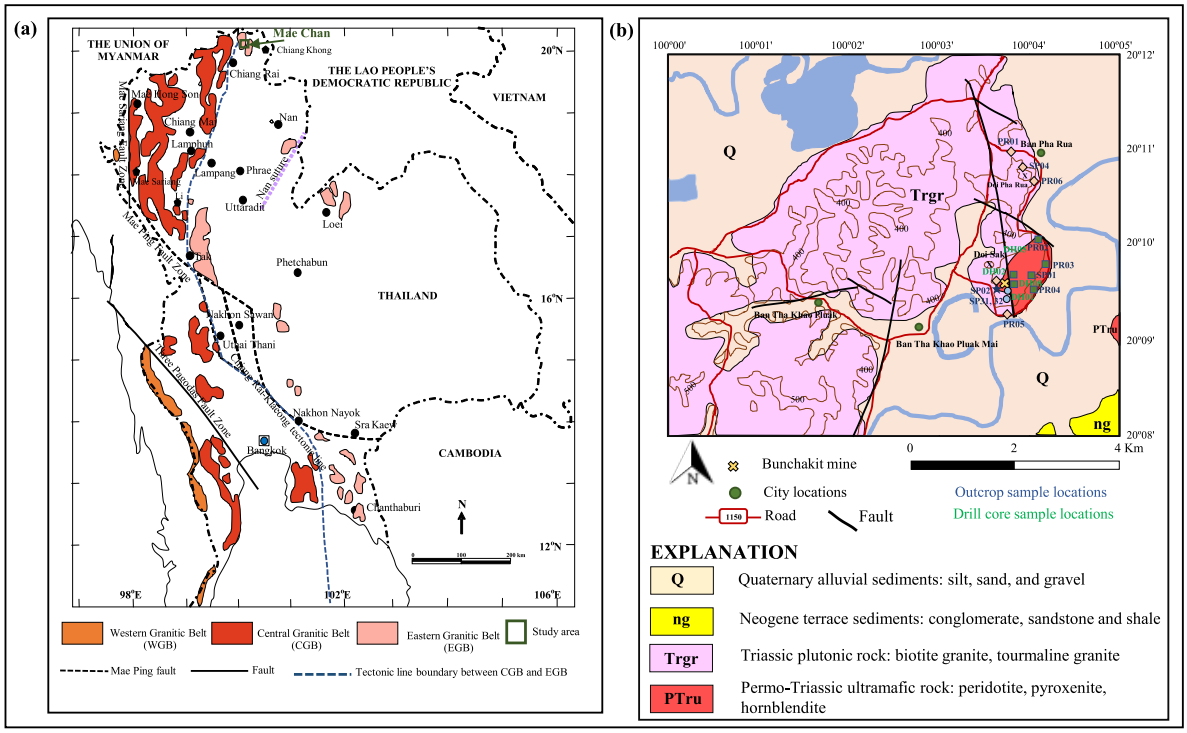

Fig. 1 (a) Map showing the distribution of western, central main range, and eastern granitic belts in Thailand, and tectonic line boundary, modified from Moley [7], Searle et al [8], Qian et al [9], and Jundee et al [10], and study location, and (b) geological map of the study area, modified from DMR [20].

sist of granite, granodiorite, and monzodiorite, which are related to metal minerals such as ilmenite and magnetite. Their whole-rock geochemistry is calc-alkaline, metaluminous, and I- to A-type. Zircon U-Pb dating of granite yields ages of 208–226 Ma (Late Triassic), corresponding to the collision of Sibumasu and Indochina terranes, and 55 Ma (Eocene), likely related to the collision of the Indian and Eurasian continents [13–18].

The study area covers Doi Pha Rua and Doi Sak, Tha Khao Pluek Sub-District, Mae Chan District, Chiang Rai Province. Geological data of the study area and vicinity, compiled by Braun and Hahn [19], reported the Lower Carboniferous stressed granite (G-h) and Quaternary sediments (Q). However, Department of Mineral Resources (DMR) [20] reported the occurrences of Triassic granite (Trgr), Permo-Triassic ultramafic rocks (peridotite, pyroxene, serpentinite, and hornblendite) (PTru), and Quaternary sediments (Q) (Fig. 1b). According to DMR [20], the Triassic igneous rock is part of the Mae Chan pluton and is classified as part of EGB. The Mae Chan pluton was divided into two sub-groups, i.e., Chatchai and Nang Lae subgroups. The Chatchai subgroup was in the western part of the pluton, composed of slightly porphyritic stressed granite with biotite phenocrysts. The Nang Lae subgroup is distributed east of the pluton and consists of medium- to coarse-grained porphyritic granite with K-feldspar, biotite, and hornblende phenocrysts. The aim of this study is to petrochemically characterize the felsic to mafic plutonic rocks in the eastern part of Mae Chan area, which are informative regarding tectonic environments of formation and relationships. This information will be useful for igneous database of Thailand and vicinity and provides some certain clues for interpretating the tectonic evolution of Thailand.

MATERIALS AND METHODS

Sample collection and selection

A number of felsic to mafic intrusive rock samples were carefully selected to obtain least-altered samples from both outcrops and drill cores. The studied igneous rocks were collected from both outcrops (11 samples) and drill cores (9 samples) in the Banchakit mine area (Fig. 1). The outcrop samples are SP01, SP02, SP31, SP32, SP04, MCPR01, MCPR02, MCPR03, MCPR04, MCPR05, and MCPR06, whereas the core samples are DH011, DH012, DH021, DH022, DH051, DH052, DH053, DH054, and DH08. The least-altered samples generally exclude those with extensive development of mesoscopic domains of secondary minerals, such as silicied quartz, epidote, and chlorite; well-developed foliation or mineral layering; xenocrysts; and xenoliths totaling more than 5 modal%.

Sample preparation

The selected rock samples were prepared as thin sections for petrographic study, stained for modal analysis, and powdered for whole-rock chemical analysis. For convenience, the rock slabs of felsic rocks were stained to differentiate K-feldspar from plagioclase using amaranth and sodium cobaltinitrite solutions [21]. Modal analysis was performed on stained medium-grained felsic rock slabs, unstained medium-grained mafic rock slabs, and thin sections. In case of fine-grained mafic rocks, modal analysis was performed under the petrographic microscope. The modal analysis carried out in this study was based on 400 counts, and the results are listed in Table S1.

The least-altered samples were prepared as sample powder for whole-rock chemical analysis by splitting into conveniently sized fragments and then crushing them into small chips, using a Rocklabs Hydraulic Splitter/Crusher. Approximately 50–80 g of cautiously selected and cleaned chips were pulverized for a few minutes using an automatic laboratory disc mill, model Scheibenschwingmühle-TS1000 (Mülheim, Germany), installed at the Department of Geological science, Chiang Mai university, Chiang Mai, Thailand.

Analytical techniques

The sample powders were chemically analyzed for major oxides, trace elements, rare-earth elements (REEs), and loss on ignition (LOI). Rock-powdered samples were prepared as fused glass beads and pressed powders. Chemical analyses of major and minor oxides (SiO_2, TiO_2, Al_2O_3, total iron (FeO and Fe_2O_3) as FeO*, MnO, MgO, CaO, Na_2O, K_2O, and P_2O_5) and some certain trace elements (Ba, Rb, Sr, Y, Zr, Nb, Ni, V, Sc, Cr, and Th) were carried out using a PANalytical Zetium X-ray fluorescence (XRF) spectrometer (wavelength dispersive system), model Zetium PW5400 (Almelo, Netherlands), installed at the Science Laboratory for Education Division, Kanchanaburi campus, Mahidol University, Thailand. The standards used were the set of SARM standards (GS-N, MA-N, and BE-N) [22] and GSJ Igneous standards (JG-2, JB-2a, and JB-3) [23] with Ausmon111 Drift Monitor. These major elements were measured from fused glass beads prepared with 0.5 g of powdered sample and 6.5 g of mixing materials (anhydrous lithium tetraborate ($Li_2B_4O_7$) 49.75%, lithium metaborate ($LiBO_2$) 49.75%, and lithium bromide (LiBr) 0.5%) and fused with fusion machine, model M4 (Quebec, Canada). Trace elements were measured from pressed powders prepared with 4 g of sample powder and 1 g of XRF binder (Licowax, Bedburg-Hua, Germany). Detection limits for Ba are 50 ppm, whereas those for Rb, Sr, Ni, V, Cr, and Zr are 10 ppm, and those for Y, Nb, Sc, and Th are 5 ppm. Ignition loss was determined by heating approximately 1 g of powdered samples at 1000 °C for 12 h for mafic rocks and at 800 °C for 8 h for felsic rocks. These procedures were carried out at the Department of Geological Science, Chiang Mai University, Chiang Mai, Thailand. Some certain trace elements (Th and U) and REEs (La, Ce, Pr, Nd, Sm, Eu, Gd, Tb, Dy, Ho, Er, Tm, Yb, and Lu) were determined on all the least-altered samples, using a PerkinElmer NexION® 2000 Inductively Coupled Plasma Mass Spectrometer (ICP-MS) (Waltham, USA). Solutions for ICP-MS analysis were prepared by the Microwave digestion technique. The standards used in the ICP-MS analysis were the international standard JA-1 and JB-1a. These procedures were carried out at DMR. The chemical concentrations of the rocks are listed in Table S2.

RESULTS AND DISCUSSION

Field occurrence and relations

The igneous rocks presented in this study are from the eastern part of Mae Chan District, Chiang Rai Province. They are composed mainly of granitic rocks, with minor gabbro and mafic dikes.

Rock nomenclature and assessment of least-altered nature

Almost all of the studied least-altered plutonic samples are medium-grained, except for sample DH012 that is fine-grained, and have modal mafic minerals of less than 90%. They have been plotted in terms of modal quartz, alkali feldspar, and plagioclase to name the rocks according to the IUGS classification of plutonic rocks [24] (Fig. 2). The diagram shows that the studied samples include monzogranite, granodiorite, and diorite/gabbro. The diorite/gabbro samples have SiO_2 contents of less than 52 wt%, implying that the rocks are gabbro. Owing to the fine-grained nature of sample DH012, the name "microgabbro" has been assigned to the sample. The Group IV microgabbro seems to be a portion of dike in the main granitic body.

The alteration box plot of Large et al [25] (Fig. 3) was applied to the studied samples to assess their least-altered nature. The data for major oxides, in terms of weight%, were used to calculate the Ishikawa alteration index (AI) and chlorite-carbonate-pyrite index (CCPI), following the equations.

$$\mathrm{AI} = \frac{100(\mathrm{MgO} + \mathrm{K_2O})}{\mathrm{FeO} + \mathrm{K_2O} + \mathrm{MgO} + \mathrm{Na_2O}}$$

$$\mathrm{CCPI} = \frac{100(\mathrm{FeO} + \mathrm{MgO})}{\mathrm{FeO} + \mathrm{K_2O} + \mathrm{MgO} + \mathrm{Na_2O}}$$

The result shows that the studied monzogranite and granodiorite lie almost entirely in the field of least-altered felsic-intermediate rocks; only one sample is outside the field, although it is very close to the field boundary of least-altered felsic-intermediate rocks. This phenomenon is also true for the studied tonalite, which is mainly in the field of least-altered

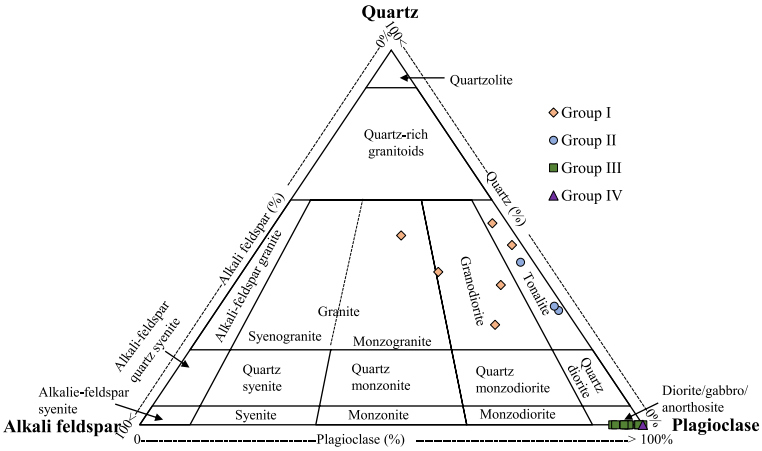

Fig. 2 IUGS classification of plutonic rocks [24], showing positions of the studied least-altered plutonic rocks.

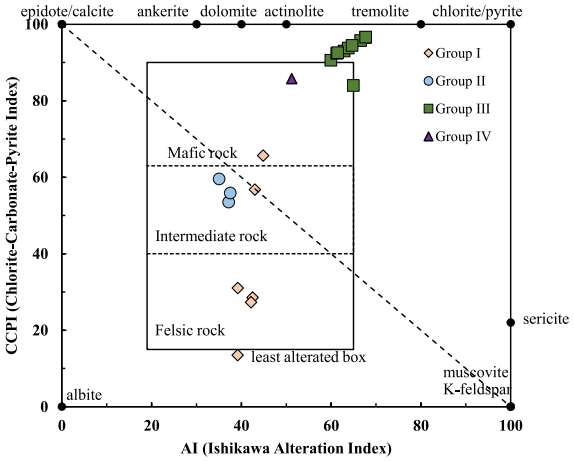

Fig. 3 The alteration box [25] for volcanic rock to evaluate alteration intensity of the studied least-altered plutonic rocks.

intermediate rocks, but one sample is outside and very close to the field boundary of intermediate-mafic rocks. The studied mafic rocks (gabbro and microgabbro) form a cluster overlapping the right-hand corner of the limit between least-altered and altered mafic rocks. Only one gabbro sample and one microgabbro sample lie within the field of least-altered mafic rocks. These confirm the least-altered nature of the carefully selected samples. The appearance of gabbro outside the field of least-altered rocks may be arisen from the fact that the gabbro are cumulate rocks, i.e., they do not represent molten magma, but the diagrams were constructed using data of volcanic rocks, chemically equivalent to magma.

Magmatic groups

The studied least-altered plutonic samples have a wide range of compositions. They are acidic to basic in composition, with 46.36–73.32 wt% SiO_2, and seem to form a board, continuous fractionation trends on $Na_2O + K_2O$ versus SiO_2 [26, 27] (Fig. 4a) and AFM [27] (Fig. 4b) plots, suggestive of co-magmatic origin. The chondrite-normalized REE patterns of the rocks, however, do not support the co-magmatic origin. Therefore, magmatic grouping has been carried out, based on occurrences, petrography, and geochemistry, in particular chondrite-normalized REE and N-MORB normalized multi-element patterns. The presented least-altered rock samples may be divided into four magmatic groups: Group I monzogranite, granodiorite, and tonalite; Group II tonalite; Group III cumulate gabbro; and Group IV microgabbro. Petrography, geochemistry, and petrotectonics of Groups I, II, and IV magmatic rocks are individually discussed below. To avoid ambiguities related to the chemical compositions of molten magma, Group III cumulate gabbro is discussed based on petrography and geochemistry only.

Petrography

Group I monzogranite, granodiorite, and tonalite

Group I granitic rocks comprise monzogranite (MCPR06), granodiorite (SP04 (Fig. 5a), MCPR01, and MCPR05), and tonalite (DH21 and DH22). The rock samples are medium-grained and commonly show a seriate texture. The essential constituents of these rocks include 24–48 modal% quartz, 25–51 modal% plagioclase, and 1–22 modal% K-feldspar. Their common accessory minerals are biotite (1–24 modal%), muscovite (trace-6 modal%), titanite (trace-4 modal%), opaque mineral (trace-1 modal%), apatite (trace), and zircon (trace). Hornblende is rarely detected in sample MCPR01, and garnet is present in samples MCPR01 and MCPR05. Sieve-textured staurolite is also sporadically observed in sample MCPR05. Plagioclase is euhedral–subhedral, zoned, and slightly altered to sericite. Quartz is anhedral and forms consertal-textured clusters, interstitial to other minerals. K-feldspar is anhedral–subhedral and

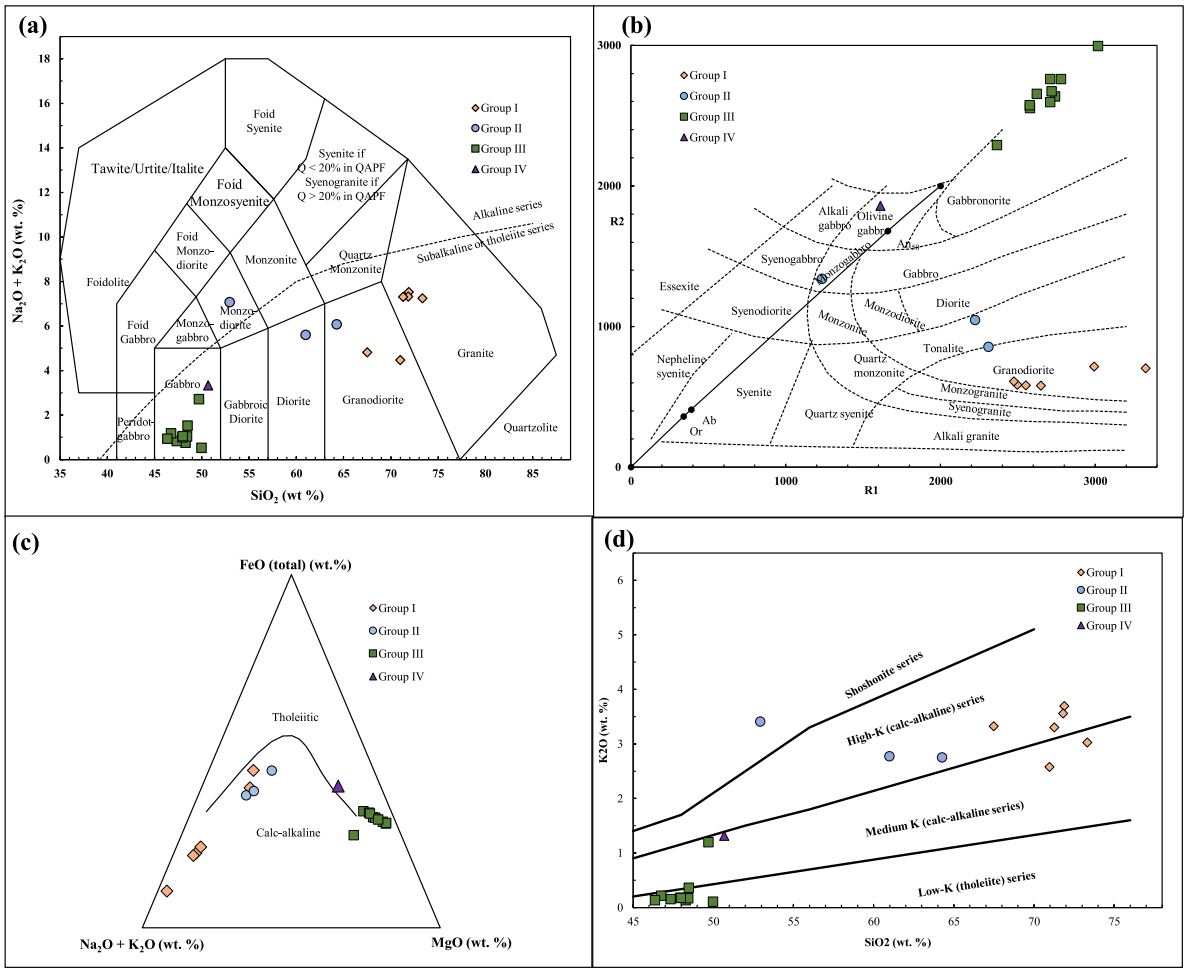

Fig. 4 Positions of the studied least-altered plutonic rocks in (a) TAS diagram [26] with tholeiitic–calc-alkaline line boundary of Irvine and Baragar [27], (b) R1–R2 diagram [30], (c) AFM diagram [27], and (d) K_2O versus SiO_2 diagram [31].

perthitic textured and occurs as an interstitial mineral. Biotite and muscovite are subhedral; the former exhibits yellowish brown to dark brown pleochroism and increases in abundance from monzogranite to tonalite. Hornblende is subhedral and generally displays yellow to pale green pleochroism. The wide compositional range from tonalite to monzogranite and the presence of titanite and hornblende are the petrographic characteristics of I-type granitic rocks [28]. The accessory staurolite in granite has been reported to occur in an extremely narrow interval of T–P conditions (T∼475–410 °C and P∼1.8–1.4 kbar), at a relatively low K activity ($< 10^{-3}$) and a high Fe activity (10^{-3}) [29].

Group II tonalite

Group II rocks (SP31, SP32, and DH011 (Fig. 5b)) are all tonalite. They are seriate-textured, medium-grained rock, consisting essentially of plagioclase (42–58 modal%), quartz (26–34 modal%), and K-feldspar (1–2 modal%), with common accessory biotite (14–17 modal%), muscovite (trace), titanite (trace), opaque minerals (trace), and zircon (trace). Garnet has been observed in small amount in sample DH011, and apatite has been occasionally detected in samples DH011 and SP31. Plagioclase is euhedralsubhedral and moderately altered to sericite. Quartz is anhedral, consertal-textured, and interstitial to other minerals and commonly exhibits a consertal texture. K-feldspar is anhedralsubhedral and occurs as an interstitial mineral. Biotite and muscovite have subhedral outlines. The former exhibits yellowish brown to dark brown pleochroism and is highly altered to chlorite.

Group III cumulate gabbro

Group III cumulate gabbro includes samples DH051, DH052, DH053, DH054, DH08, SP01 (Fig. 5c), SP02, MCPR02, MCPR03, and MCPR04. These rock samples are medium-grained, with seriate and orthocumulus textures. Their major constituents are 35–60

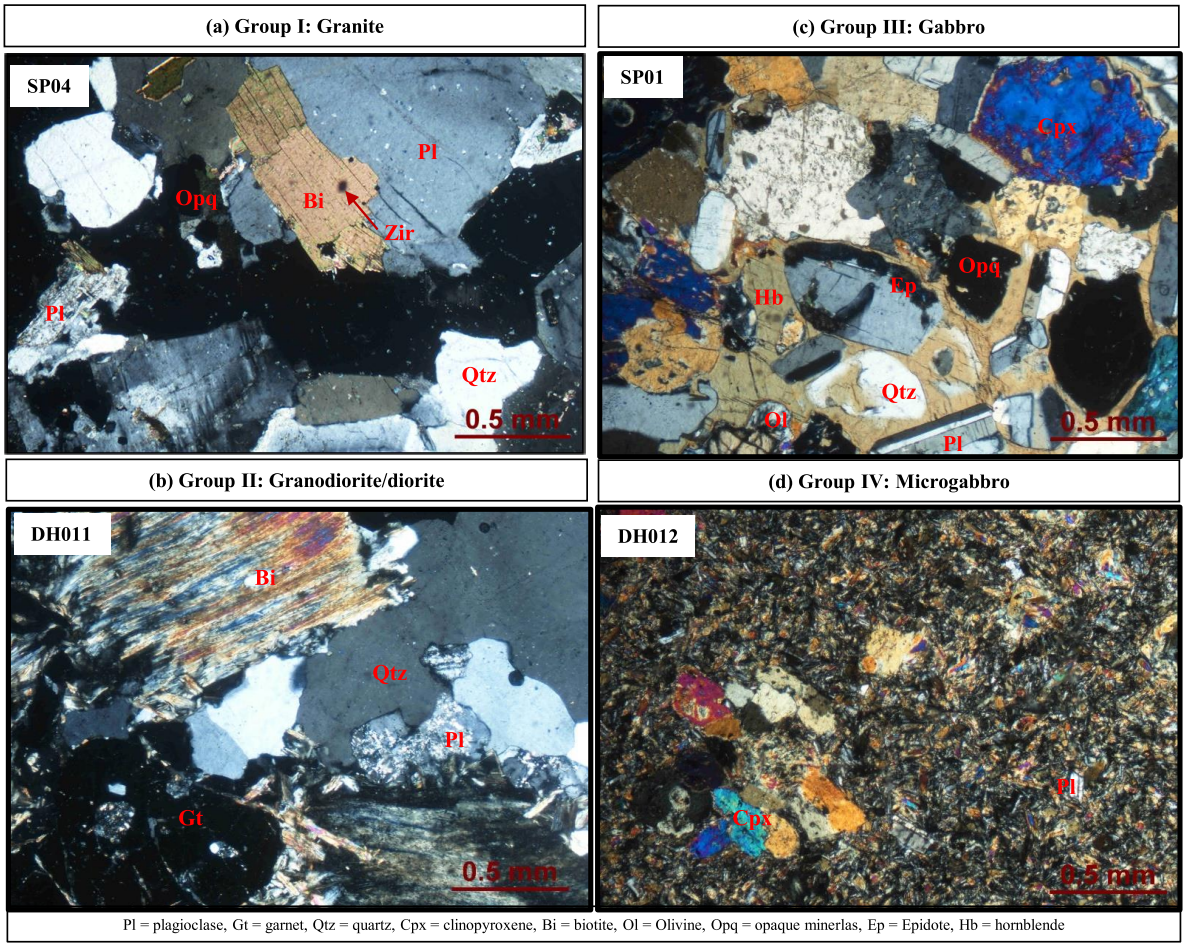

Fig. 5 The photomicrographs of representative rock samples: seriated texture of (a) Group I granite and (b) Group II granodiorite/diorite, (c) cumulated texture of Group III gabbro, and (d) porphyritic texture of Group IV microgabbro.

modal% plagioclase and may include clinopyroxene and hornblende, while minor constituents may include K-feldspar, olivine, titanite, biotite, and opaque minerals. Clinopyroxene and hornblende in some samples are present as minor constituents (Table S1). The plagioclase grains have An-content in a range of labradorite by the Michel-Levy method and show anhedral to subhedral outlines. They are slightly altered to sericite and clay minerals. Clinopyroxene and hornblende have anhedral outlines. Hornblende has pale brown to pale green pleochroism and may contain corroded clinopyroxene cores and be interstitial and poikilitic. Olivine has anhedral outlines and are moderately altered to iddingsite.

Group IV microgabbro

As its name denotes, Group IV microgabbro (DH012, Fig. 5d) is a microporphyritic, fine-grained, basic rock, with plagioclase and clinopyroxene microphenocrysts, as well as clinopyroxene glomerocrysts. The groundmass consists mainly of plagioclase and clinopyroxene, with minor titanite and opaque minerals. All the mineral constituents are mainly subhedral. Plagioclase is slightly altered to sericite and clay minerals, while clinopyroxene is slightly pseudomorphed by hornblende.

Geochemistry

Group I monzogranite, granodiorite, and tonalite

Group I rocks are subalkaline/tholeiitic granite and granodiorite on total alkalis–SiO_2 plot (Fig. 4a) [26, 27] and granodiorite on R1–R2 diagram plot (Fig. 4b) [30]. These rocks form a linear fractionation trend, caused by removal of Fe-Mg minerals, in the calc-alkaline field of AFM plot (Fig. 4c) [27]. They have medium-K to high-K, calc-alkaline signatures on K_2O versus SiO_2 plot (Fig. 4d) [31]. In terms of molar $Al_2O_3/Na_2O + K_2O$ and $Al_2O_3/CaO + Na_2O + K_2O$, Group I medium-K transitional to high-K, calc-alkaline rocks are all peraluminous, as shown in Fig. 6a [32]. Their tonalite end members appear to be S-type granite, while the more felsic granodiorite

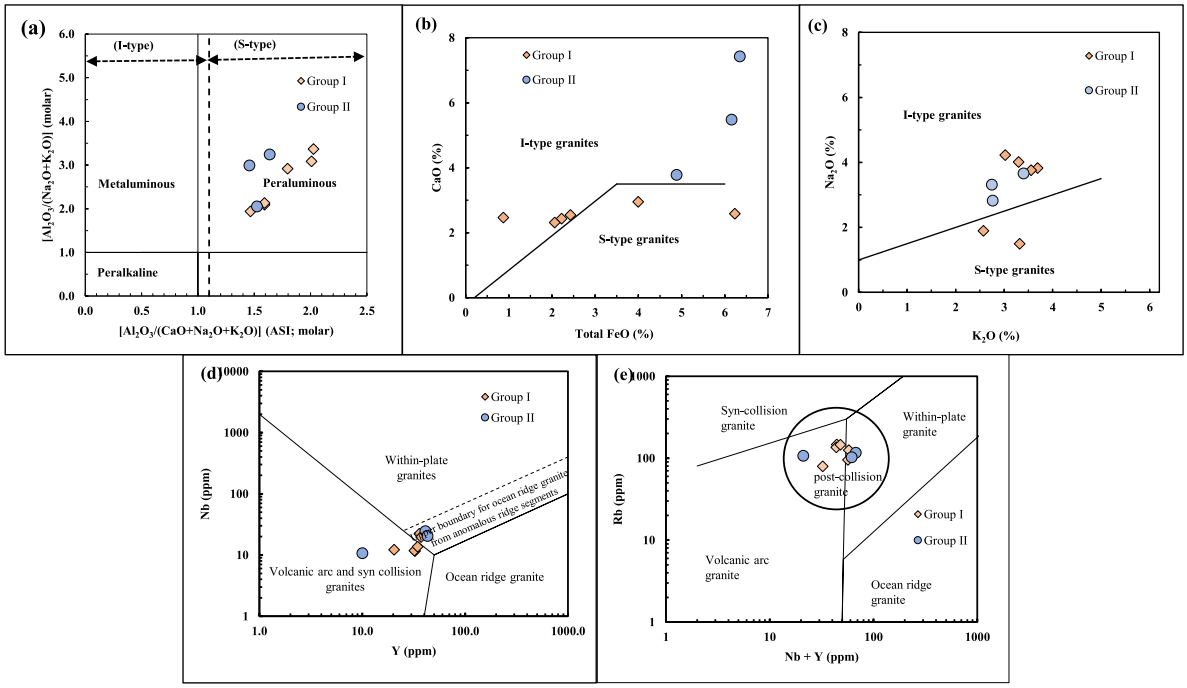

Fig. 6 Group I felsic rock and Group II felsic to intermediate rock plotted in (a) A/NK versus A/CNK [32], (b) CaO versus FeO (total) [31], (c) Na_2O versus K_2O [33], (d) Nb versus Y [36], and (e) Rb versus Nb + Y [36] diagrams.

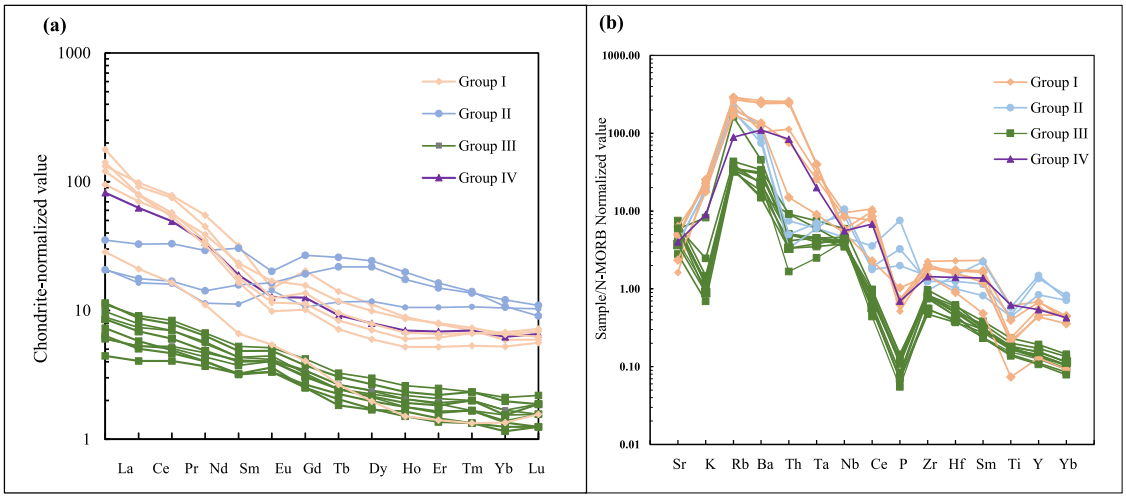

Fig. 7 (a) Chondrite-normalized REE [34] and (b) N-MORB normalized multi-element [35] patterns of the studied least-altered plutonic rocks.

and monzogranite are I-type (Fig. 6b,c) [30, 33]. The medium-K transitional to high-K, calc-alkaline series of Group I rocks is strongly supported by their chondrite-normalized REE patterns, which have relatively flat heavy REE (HREE) from Yb to Dy and light REE (LREE) enrichment from Dy to La (Fig. 7a) [34]. The values for chondrite normalized Dy/Yb ((Dy/Yb)cn) and La/Dy ((La/Dy)cn) are 1.04–1.88 and 9.58–22.57, respectively. They all show negative Eu anomalies, resulting from plagioclase fractionation.

Group II tonalite

Group II rocks are diorite and monzodiorite on total alkalis–SiO_2 plot (Fig. 4a) and tonalite-monzogabbro on R1–R2 diagram (Fig. 4b). The rocks are tholeiitic transitional to alkaline on total alkalis–SiO_2 plot (Fig. 4a), calc-alkaline on AFM plot (Fig. 4c), and high-K calc-alkaline to shoshonitic rocks on SiO_2 versus K_2O plot (Fig. 4d). The plots of chondrite-normalized REEs (Fig. 7a [34]) and N-MORB normalized multi-

elements (Fig. 7b [35]) are, however, not in agreement with the suggestion of a calc-alkaline series. The chondrite-normalized REE patters of Group II rocks are slightly enriched in LREE (chondrite-normalized La/Yb (La/Yb)cn = 1.71–3.27), typical of tholeiitic series. They show a positive Eu anomaly in the earlier stage and a negative Eu anomaly in the later stage of fractionation. The absence of Nb anomaly in N-MORB normalized multi-element patterns of Group II tonalite is not characteristic of subduction-related magma. Therefore, the rocks could not be calc-alkaline or shoshonitic. Chemically, Group II tonalite is peraluminous, similar to Group I tonalite (Fig. 6a), but it is I-type, different from Group I tonalite, which is S-type (Fig. 6b,c). The existence of titanite in Group II tonalite agrees with the characteristic of I-type granitic rocks.

Group III cumulate gabbro

The cumulate gabbro has been formed by accumulation of minerals crystallized earlier from molten magma. Therefore, the rock does not have chemical compositions equivalent to magma and will not be discussed about tectonic environment of formation. Group III gabbro contains SiO_2 in a range of 46.36–49.98 wt%, which are gabbro on total alkalis–SiO_2 (Fig. 4a) and gabbronorite on R1–R2 diagram (Fig. 4b). They are tholeiitic in chemical compositions, as shown by their positions on total alkalis–SiO_2 (Fig. 4a), AFM (Fig. 4c), and K_2O versus SiO_2 (Fig. 4d) plots. Their chondrite-normalized REE patterns show LREE enrichment, with (La/Yb)cn = 3.30–7.06 (Fig. 7a), typical of tholeiite from anorogenic environments. The patterns also show positive Eu anomalies, resulting from plagioclase accumulation. They do not show negative Nb anomalies in N-MORB normalized multi-element patterns (Fig. 7b).

Group IV microgabbro

Only one sample of Group IV microgabbro has been recognized, which is insufficient to draw a meaningful conclusion and discussion about the tectonic environment of formation. Group IV is gabbro on total alkalis–SiO_2 (Fig. 4a) and olivine gabbro on R1–R2 diagram (Fig. 4b). However, it appears to be either tholeiitic or calc-alkaline on total alkalis–SiO_2 (Fig. 4a), AFM (Fig. 4c), and K_2O versus SiO_2 (Fig. 4d) plots. In case of calc-alkaline rock, the rock is transitional between medium-K and high-K affinities based on K_2O and SiO_2 contents (Fig. 4d). The transitional medium-K to high-K, calc-alkaline affinity is strongly supported by its chondrite-normalized REE pattern (Fig. 7a). The pattern shows relatively flat HREE from Yb to Dy ((Dy/Yb)cn = 1.28) and light REE enrichment from Dy to La ((La/Dy)cn = 10.32), similar to the patterns of Group I granitic rocks. It sits among those of Group I granodiorite (Fig. 7a), signifying that they are not co-magmatic.

Petrotectonics

Normalized multi-element diagrams, which use a group of some certain elements incompatible and compatible with typical mantle mineralogy, are a powerful tool in determining tectonic setting of formation. The concentrations of large-ion lithophile elements (LILE), e.g., Cs, Rb, K, Ba, Sr, and Eu, may be a function of fluid-phase behavior, while those of high-field strength elements (HFSE), e.g., Y, Hf, Zr, Ti, Nb, and Ta, are controlled by the chemistry of source and the crystal/melt processes. In different tectonic environments with different physical conditions and mineral assemblages, the order of element incompatibility may change significantly. Chondrite-normalized REE patterns are used considerably in petrotectonics, using chondrite-normalizing values of Taylor and Gorton [34]. The normalized multi-element diagram used in this account is N-MORB normalized, established by Sun and McDonough [35].

Group I rocks exhibit wide compositional range from tonalite to monzogranite. The presence of biotite-muscovite is the petrographic characteristics of S-type granitic rocks, whereas titanite and hornblende are characteristics of I-type granitic rocks [28]. The transition from medium-K to high-K calc-alkaline rocks is the feature of volcanic arc magma rather than oceanic island-arc magma. Their tonalite end members appear to be S-type granite, while the more felsic granodiorite and monzogranite are I-type form a cluster in the fields of either orogenic or non-orogenic environment on Nb versus Y (Fig. 6d) and Sr versus Nb + Y (Fig. 6e) plots [36]. The positions of these rocks in Fig. 6e, however, are fit well to those of a post-orogenic environment. REE patterns show negative Eu anomalies. The N-MORB normalized multi-element patterns (Fig. 7b) show LILE enrichment and negative Nb anomalies relative to Th and Ce, which are significant signatures of subduction-related magma [37].

Group II rocks are tonalite. The existence of titanite agrees with the characteristics of I-type granitic rocks. Group II appear to have formed in arc and within-plate environments, as indicated by Nb versus Y (Fig. 6d) and Sr versus Nb + Y (Fig. 6e) plots. The REE patters are typical of tholeiitic series and do not show a negative Eu anomaly (Fig. 6b). Their N-MORB normalized multi-element patterns support the within-plate environment. The appearance of an arc environment might be due to the magma having formed in the tectonic environment transitional from arc to within-plate, i.e., post-collision, as shown in Fig. 6e.

Group III cumulate gabbro is discussed in view of petrography and geochemistry only, to avoid ambiguities involved in the chemical compositions of molten magma. Group IV microgabbro has an insufficient sample to draw a meaningful conclusion and discussion about the tectonic environment of formation.

Although the tectonic environments of individual

magmatic groups have been determined, the ages of the rocks and their relationships remain uncertain. However, the Mae Chan granitic rocks (Groups I and II) have a zircon U-Pb age of 226+3 Ma (Late Triassic) [13]. The gabbro/microgabbro (Groups III and IV) were inferred to be Permo-Triassic [20]. The contacts between the granitic rocks and gabbro/microgabbro remain obscure in the field, and the geochemical relationship does not relate to a faulted contact. Based on petrography, geochemistry and field relationship, Mae Chan granitic plutons are assigned to be part of EGB of Southeast Asia, which sporadically continues southward to Tak batholith [38] and indicates the magmatism along the boundary between Sukhothai Arc and Inthanon Zone [17]. In addition, the mafic-ultramafic rocks can be observed in these belts [39, 40].

CONCLUSION

The Mae Chan plutonic rocks are dominantly felsic with minor intermediate to mafic plutonic and mafic volcanic rocks. These rocks may be divided into 4 groups. Groups I and II are isotropic rocks. The chemical compositions are equivalent to those of magma and could yield information concerning the tectonic environment of formations. Group III has been formed by the accumulation of crystals from magma, by either sinking and floating, i.e., not chemically equivalent to magma. One Group IV sample is isotropic, but meaningless for interpretation. Group I compositionally ranges from S-type tonalite with minor biotite and muscovite to I-type granodiorite and monzogranite with minor biotite, titanite, and hornblende. Group I belongs to the medium-K transitional to high-K calc-alkaline series, is peraluminous, shows LILE enrichments, and has negative Nb anomalies, typical of magmas formed at active continental margins. Group II is I-type tonalite with minor titanite, peraluminous, and tholeiitic in composition, and the absence of negative Nb anomalies implies that it might have formed in an anorogenic/post-collision environment. Group III is gabbro/gabbronorite that shows cumulate texture and belongs to the tholeiite series and orogenic environments, characterized by positive Eu anomalies, indicative of plagioclase accumulation. The Mae Chan granitic pluton is part of EGB and can be correlated with the Tak pluton, indicating magmatism along the boundary between the Sukhothai Arc and Inthanon Zone.

Appendix A. Supplementary data

Supplementary data associated with this article can be found at https://dx.doi.org/10.2306/scienceasia1513-1874.2025.s026.

Acknowledgements: The authors would like to acknowledge financial support from the Faculty of Science, Chiang Mai University; Igneous Rocks and Related Ore Deposits Research Unit, Department of Geological Sciences, Faculty of Science, Chiang Mai University; Geoscience Program, Mahidol University, Kanchanaburi campus; and Department of Mineral Resources.

REFERENCES

1. Cobbing EJ, Mallick DIJ, Pitfield PEJ, Teoh LH (1986) The granites of the Southeast Asian Tin Belt, *J Geol Soc London* **143**, 537–550.
2. Charusiri P, Clark AH, Farrar E, Archibald D, Charusiri B (1993) Granite belts in Thailand: evidence from the $^{40}Ar/^{39}Ar$ geochronological and geological syntheses. *J Southeast Asian Earth Sci* **8**, 127–136.
3. Linnen RL (1998) Depth of emplacement, fluid provenance and metallogeny in granitic terranes: A comparison of western Thailand with other tin belts. *Miner Depos* **33**, 461–476.
4. Putthapiban P (2002) Geology and geochronology of igneous rocks of Thailand. In: *Proc Symp Geol Thailand*, Department of Mineral Resources, Bangkok, pp 261–283.
5. Charusiri P, Pungrassami T, Sinclair G (2006) Classification of rare-earth element (REE) deposit in Thailand: A genetic model. *J Geol Soc Thailand* **1**, 57–66.
6. Phountong K, Salam A, Manaka T (2020) Petrochemistry of granite from Takua Pit Thong area, Ratchaburi, Thailand. *Bull Earth Sci Thailand* **12**, 15–29.
7. Morley CK (2002) A tectonic model for the Tertiary evolution of strike-slip faults and rift basins in SE Asia. *Tectonophysics* **347**, 189–215.
8. Searle MP, Whitehouse MJ, Robb LJ, Ghani AA, Hutchison CS, Sone M, Ng SWP, Roselee MH, et al (2012) Tectonic evolution of the Sibumasu–Indochina terrane collision zone in Thailand and Malaysia: constraints from new U-Pb zircon chronology of SE Asian tin granitoids. *J Geol Soc* **169**, 489–500.
9. Qian X, Feng Q, Wang Y, Zhao T, Zi JW, Udchachon M, Wang Y (2017) Late Triassic post-collisional granites related to Paleotethyan evolution in SE Thailand: geochronological and geochemical constraints. *Lithos* **286**, 440–453.
10. Jundee PK, Phanbuppha S, Jamsai T, Phajuy B (2022) Petrochemistry of granitic rock in Tha Pai area, Mae Hi Sub-district, Pai District, Mae Hong Son Province, Thailand. *Songklanakarin J Sci Technol* **44**, 1427–1433.
11. Ghani AA, Searle M, Robb L, Chung S (2013a) Transitional I S type characteristic in the Main Range granite, peninsular Malaysia. *J Asian Earth Sci* **76**, 225–240.
12. Jundee PK, Chaiwchan S, Inthacharoensarn S, Phajuy B, Nontarak P (2024) Petrochemistry and tectonic setting of the Phroa–Wiang Pa Pao granitic rocks, Chiang Mai, and Chiang Rai Provinces, Central Granitic Belt of Thailand. *Trends Sci* **21**, 8055.
13. Wang Y, He H, Cawood PA, Srithai B, Feng Q, Fan W, Yuzhi Z, Qian X (2016) Geochronology, elemental and Sr-Nd-Hf-O isotopic constraints on the petrogenesis of the Triassic post-collisional granitic rocks in NW Thailand and its Paleotethyan implications. *Lithos* **266**, 264–286.
14. Ghani AA, Chung CH Lo, Chung SL (2013) Basaltic dykes of the Eastern Belt of Peninsular Malaysia: the effects of the difference in crustal thickness of Sibumasu and Indochina. *J Asian Earth Sci* **77**, 127–139.
15. Nualkhao P, Takahashi R, Imai A, Charusiri P (2018)

Petrochemistry of granitoids along the Loei Fold Belt, Northeastern Thailand. *Resour Geol* **68**, 1–30.
16. Fanka A, Nakapadungrat S (2018) Preliminary study on petrography and geochemistry of granitic rocks in the Khao Phra–Khao Sung area, Amphoe Nong Bua, Changwat Nakhon Sawan, Central Thailand. *Bull Earth Sci Thailand* **9**, 55–68.
17. Qian X, Wang Y, Zhang Y, Wang Y, Senebouttalath V (2020) Late Triassic post-collisional granites related to Paleotethyan evolution in northwestern Lao PDR: geochronological and geochemical evidence. *Gondwana Res* **84**, 163–176.
18. Uchida E, Nagano S, Niki S, Yonezu K, Saitoh Y, Shin K, Hirat T (2020) Geochemical and radiogenic isotopic signatures of granitic rocks in Chanthaburi and Chachoengsao provinces, southeastern Thailand: implications for origin and evolution. *J Asian Earth Sci X* **8**, 100111.
19. Braun EV, Hahn L (1976) Geological Map of Northern Thailand. 1:250,000 (Chiang Rai). Department of Minerals and Resources, Bangkok, Thailand.
20. Department of Minerals and Resources (2007) Geological Map of Chiang Rai Province, Department of Minerals and Resources, Bangkok, Thailand.
21. Hutchison CS (1973) *Laboratory Handbook of Petrographic Techniques*, John Wiley and Sons, Inc., New York, USA.
22. Govindaraju K, Roelandts I (1993) Second report on the first three GIT-IWG rock reference samples: anorthosite from Greenland, AN-G; basalt DÈssey-la-Côte, BE-N; granite De Beauvoir, MA-N. *Geostand Newsl* **17**, 227–294.
23. Imai N, Terashima S, Itoh S, Ando A (1995) 1994 Complication of analytical data for minor and trace elements in seventeen GSJ geochemical reference samples, "Igneous rock series". *Geostand Newsl* **19**, 135–213.
24. Streckeisen A (1976) To each plutonic rock its proper name. *Earth Sci Rev* **12**, 1–33.
25. Large RR, Gemmell JB, Paulick H, Huston DL (2001) The alteration box plot: A simple approach to understanding the relationship between alteration mineralogy and lithogeochemistry associated with volcanic-hosted massive sulfide deposits. *Econ Geol* **96**, 957–971.
26. Middlemost EAK (1994) Naming materials in the magma/igneous rock system. *Earth Sci Rev* **37**, 215–224.
27. Irvine TNJ, Baragar WRA (1971) A guide to the chemical classification of the common volcanic rocks. *Canadian J Earth Sci* **8**, 523–548.
28. Chappell BW, White AJR (1974) Two contrasting granite types. *Pac Geol* **8**, 173–174.
29. Gordienko VV, Ponomareva NI, Kretser, YuL (2012) Staurolite and associated minerals from rare-metal granite pegmatites. *Geol Ore Depos* **54**, 676–687.
30. De la Roche H, Leterrier J, Grande Claude P, Marchal M (1980) A classification of volcanic and plutonic rocks using R1–R2 diagrams and major element analyses-its relationships and current nomenclature. *Chem Geol* **29**, 183–210.
31. Peccerillo A, and Taylor SR (1976) Geochemistry of Eocene calc-alkaline volcanic rocks from the Kastamonu area, northern Turkey. *Contrib Mineral Petrol* **58**, 63–81.
32. Maniar PD, Piccoli PM (1989) Tectonic discrimination of granitoids. *Geol Soc Am Bull* **101**, 635–643.
33. Chappell BW, White AJR (2001) Two contrasting granite types: 25 years later. *Aust J Earth Sci* **48**, 489–499.
34. Taylor SR, Gorton MK (1977) Geochemical application of spark-source mass spectrometry; III: Element sensitivity, precision and accuracy. *Geochim Cosmochim Acta* **41**, 1375–1380.
35. Sun SS, McDonough WF (1989) Chemical and isotopic systematics of oceanic basalt: Implications for mantle composition and processes. *Geol Soc Publ* **42**, 313–345.
36. Pearce JA, Harris NBW, Tindle AG (1984) Trace element discrimination diagrams for the tectonic interpretation of granite rocks. *J Petrol* **25**, 956–983.
37. Baier J, Audétat A, Kepple H (2008) The origin of the negative niobium tantalum anomaly in subduction zone magmas. *Earth Planet Sci Lett* **267**, 290–300.
38. Phajuy B, Singtuen V (2019) Petrochemical characteristics of Tak volcanic rocks, Thailand: implication for tectonic significance. *ScienceAsia* **45**, 350–360.
39. Fanka A, Tsunogae T, Daorerk V, Tsutsumi Y, Takamura Y, Endo T (2016) Petrochemistry and mineral chemistry of Late Permian hornblendite and hornblende gabbro from the Wang Nam Khiao area, Nakhon Ratchasima, Thailand: Indication of palaeo-tethyan subduction. *J Asian Earth Sci* **130**, 239–255.
40. Assawincharoenkij T, Sutthirat C, Chenrai P, Imsamut S, Charusiri P (2021) Petrogenesis of mafic-ultramafic and associated rocks along Sa Kaeo and Pattani Sutures, Thailand. *ScienceAsia* **47**, 741–750.

Appendix A. Supplementary data

Table S1 Modal analyses of the studied least-altered plutonic rocks in terms of volume%.

Group	Group I						Group II			Group IV
Sample no.	DH021	DH022	SP04	MCPR01	MCPR05	MCPR06	DH011	SP31	SP32	DH012
Quartz	35.75	40.50	23.75	38.25	34.25	48.25	33.75	26.00	27.00	nd
K-Feldspar	1.50	2.25	14.25	19.00	8.75	21.75	2.00	1.25	1.50	nd
Plagioclase	37.25	32.50	51.00	36.50	48.75	25.50	42.00	58.00	56.75	34.00
Clinopyroxene	nd	nd	nd	nd	nd	nd	nd	nd	nd	65.75
Hornblende	nd	nd	nd	0.25	tr	nd	nd	nd	nd	nd
Titanite	tr	tr	3.50	3.75	3.75	2.00	tr	tr	tr	tr
Garnet	nd	nd	nd	tr	tr	nd	5.00	nd	nd	nd
Biotite	17.50	24.50	6.75	1.75	4.00	1.50	17.25	14.25	14.75	nd
Muscovite	6.50	tr	tr	tr	tr	tr	tr	tr	tr	nd
Apatite	tr	tr	tr	0.50	0.25	0.25	tr	0.50	nd	nd
Opaque mineral	1.50	0.25	0.75	tr	tr	0.75	tr	tr	tr	0.25
Zircon	tr	tr	tr	tr	0.25	tr	tr	tr	tr	nd
sum	100.00	100.00	100.00	100.00	100.00	100.00	100.00	100.00	100.00	100.00

	Group III									
	DH051	DH052	DH053	DH054	DH08	SP01	SP02	MCPR02	MCPR03	MCPR04
K-Feldspar	2.25	2.25	0.50	tr	2.00	0.50	1.50	1.50	1.50	2.00
Plagioclase	35.50	39.50	49.50	39.00	52.75	60.00	43.00	50.75	53.50	51.50
Clinopyroxene	42.00	51.75	35.00	43.50	12.25	12.00	13.75	3.50	7.50	3.00
Olivine	10.75	nd	1.50	tr	0.75	3.00	2.25	0.25	3.50	4.75
Hornblende	8.75	5.75	13.50	17.50	32.00	24.50	39.50	40.75	30.00	37.75
Titanite	0.25	0.75	tr	tr	tr	tr	tr	2.75	3.75	1.00
Biotite	nd	nd	nd	nd	nd	nd	nd	nd	0.25	nd
Opaque mineral	0.50	tr	tr	tr	0.25	tr	tr	0.50	tr	tr
sum	100.00	100.00	100.00	100.00	100.00	100.00	100.00	100.00	100.00	100.00

tr = trace, nd = not detected.

Table S2 Major and minor oxides, some certain trace elements, and REE of the studied least-altered plutonic rocks.

Group	Group I						Group II		
Sample no.	DH021	DH022	SP04	MCPR01	MCPR05	MCPR06	DH011	SP31	SP32
Major oxide (wt%)									
SiO_2	67.49	70.97	71.90	71.82	73.32	71.27	64.28	52.94	60.98
TiO_2	0.78	0.50	0.28	0.26	0.09	0.30	0.56	0.75	0.59
Al_2O_3	14.87	15.04	14.59	15.32	15.45	15.02	17.68	21.12	18.12
FeO*	6.24	4.00	2.22	2.06	0.87	2.43	4.89	6.35	6.16
MnO	0.11	0.07	0.13	0.12	0.08	0.14	0.24	0.15	0.33
MgO	2.97	1.87	0.78	0.69	0.25	0.86	2.10	2.60	2.08
CaO	2.59	2.95	2.43	2.31	2.46	2.54	3.78	7.43	5.48
Na_2O	1.49	1.89	3.83	3.76	4.22	4.01	3.31	3.66	2.82
K_2O	3.32	2.58	3.69	3.56	3.02	3.30	2.75	3.40	2.77
P_2O_5	0.14	0.14	0.15	0.11	0.22	0.13	0.41	1.59	0.68
LOI	2.58	1.58	0.58	0.64	0.70	0.70	2.30	1.94	0.81
Original Sum	100.22	101.45	101.29	101.40	101.39	101.97	101.95	101.95	101.33
Trace elements (ppm)									
Ba	669	865	1624	1522	806	1494	90	797	573
Rb	126	96	147	136	80	146	<10	102	87
Sr	146	211	440	435	566	457	232	426	341
Y	36	37	33	32	20	34	10	43	41
Zr	167	135	151	139	109	139	29	71	92
Nb	22	20	12	12	12	14	11	25	20
Ni	92	61	14	16	16	20	65	16	15
Cr	155	90	11	<10	<10	29	426	12	18
V	80	48	26	21	<10	27	14	62	47
Sc	16	10	8	5	<5	6	25	17	19
Th	16	12	37	38	5	34	<5	<5	<5
REE (ppm)									
La	41.70	30.00	38.10	44.70	9.00	56.00	6.60	11.10	6.50
Ce	79.90	57.30	63.90	64.80	17.10	74.50	13.30	26.60	14.40
Pr	9.07	6.44	6.20	6.67	1.91	8.71	1.86	3.83	1.96
Nd	32.80	23.30	19.30	20.80	6.60	26.80	6.80	17.50	8.50
Sm	6.10	4.49	3.17	3.45	1.27	4.28	2.15	5.85	3.03
Eu	1.07	1.22	0.71	0.83	0.39	0.90	1.03	1.45	1.18
Gd	5.25	4.07	2.63	2.92	1.05	3.54	2.76	6.94	4.97
Tb	0.69	0.58	0.35	0.41	0.13	0.47	0.57	1.27	1.07
Dy	3.62	3.23	1.94	2.30	0.64	2.56	3.83	7.91	7.10
Ho	0.65	0.63	0.38	0.44	0.11	0.49	0.77	1.45	1.27
Er	1.67	1.70	1.11	1.31	0.30	1.40	2.25	3.48	3.19
Tm	0.21	0.22	0.16	0.20	0.04	0.20	0.32	0.42	0.41
Yb	1.23	1.37	1.09	1.41	0.28	1.36	2.17	2.24	2.51
Lu	0.19	0.20	0.18	0.23	0.05	0.22	0.33	0.29	0.35

FeO* = total iron (FeO and Fe_2O_3).

Table S2 (Continued.)

Group	Group III										Group IV
Sample no.	DH051	DH052	DH053	DH054	DH08	SP01	SP02	MCPR02	MCPR03	MCPR04	DH012
Major oxide (wt%)											
SiO_2	48.29	47.34	49.98	49.70	48.48	48.45	47.94	46.76	47.98	46.36	50.67
TiO_2	0.23	0.20	0.21	0.18	0.30	0.23	0.22	0.21	0.24	0.18	0.79
Al_2O_3	12.89	16.02	13.33	19.88	18.89	19.56	18.90	21.68	21.13	20.43	15.19
FeO*	6.45	5.81	4.66	4.43	5.31	4.66	4.96	5.04	4.56	5.17	9.39
MnO	0.12	0.10	0.10	0.08	0.10	0.08	0.09	0.09	0.08	0.09	0.18
MgO	14.63	12.75	10.53	9.80	9.31	9.20	10.01	9.25	8.48	10.79	10.68
CaO	16.65	16.94	20.65	13.20	16.07	16.77	16.86	15.78	16.45	16.05	9.62
Na_2O	0.62	0.67	0.42	1.51	1.15	0.87	0.81	0.96	0.88	0.80	2.02
K_2O	0.13	0.15	0.10	1.19	0.36	0.16	0.17	0.21	0.17	0.13	1.32
P_2O_5	0.01	0.01	0.01	0.02	0.03	0.02	0.03	0.03	0.03	0.02	0.14
LOI	1.84	2.38	2.54	2.78	2.24	1.16	1.06	1.10	2.09	1.10	2.78
Original Sum	100.19	99.03	100.16	100.19	100.13	99.10	99.56	99.55	99.09	99.83	99.73
Trace elements (ppm)											
Ba	124	122	90	263	100	164	172	179	136	133	499
Rb	<10	<10	<10	75	<10	<10	<10	<10	<10	<10	37
Sr	303	330	232	474	287	511	500	680	539	540	343
Y	10	10	10	18	16	11	10	10	10	10	19
Zr	35	36	29	52	79	57	56	72	62	56	96
Nb	10	10	11	9	14	9	9	8	9	9	13
Ni	93	88	65	65	34	69	74	90	76	27	227
Cr	399	314	426	183	143	204	283	92	252	89	906
V	15	<10	14	11	93	15	13	13	17	<10	76
Sc	35	29	25	21	33	25	23	22	25	23	34
Th	<5	<5	<5	<5	<5	<5	<5	<5	<5	<5	10
REE (ppm)											
La	1.90	1.40	1.90	2.30	3.50	2.80	2.70	3.10	3.60	2.00	25.90
Ce	4.30	3.30	4.30	4.70	7.40	6.00	5.60	6.40	7.10	4.10	50.90
Pr	0.61	0.47	0.59	0.57	0.97	0.81	0.70	0.81	0.91	0.54	5.72
Nd	2.80	2.20	2.60	2.40	4.00	3.30	2.90	3.40	3.80	2.40	20.20
Sm	0.79	0.62	0.72	0.61	1.01	0.83	0.77	0.83	0.93	0.62	3.62
Eu	0.29	0.24	0.29	0.24	0.37	0.30	0.29	0.32	0.35	0.26	0.92
Gd	0.88	0.69	0.81	0.65	1.09	0.89	0.79	0.84	0.97	0.65	3.26
Tb	0.13	0.11	0.12	0.09	0.16	0.13	0.12	0.12	0.15	0.10	0.45
Dy	0.78	0.64	0.73	0.55	0.97	0.77	0.70	0.69	0.87	0.56	2.59
Ho	0.16	0.13	0.15	0.12	0.19	0.15	0.14	0.13	0.17	0.11	0.51
Er	0.44	0.35	0.40	0.31	0.53	0.41	0.39	0.34	0.47	0.29	1.46
Tm	0.06	0.05	0.05	0.04	0.07	0.06	0.06	0.05	0.07	0.04	0.21
Yb	0.35	0.28	0.32	0.26	0.44	0.35	0.32	0.29	0.41	0.24	1.30
Lu	0.06	0.04	0.05	0.04	0.07	0.05	0.06	0.05	0.06	0.04	0.21

FeO* = total iron (FeO and Fe_2O_3).